metals

MDPI

Article

Structural Relaxation and Delayed Yielding in Cyclically Sheared Cu-Zr Metallic Glasses

Nikolai V. Priezjev [1,2]

[1] Department of Civil and Environmental Engineering, Howard University, Washington, DC 20059, USA; nikolai.priezjev@howard.edu
[2] Department of Mechanical and Materials Engineering, Wright State University, Dayton, OH 45435, USA

Abstract: The yielding transition, structural relaxation, and mechanical properties of metallic glasses subjected to repeated loading are examined using molecular dynamics simulations. We consider a poorly annealed Cu-Zr amorphous alloy periodically deformed in a wide range of strain amplitudes at room temperature. It is found that low-amplitude cyclic loading leads to a logarithmic decay of the potential energy, and lower energy states are attained when the strain amplitude approaches a critical point from below. Moreover, the potential energy after several thousand loading cycles is a linear function of the peak value of the stress overshoot during startup continuous shear deformation of the annealed sample. We show that the process of structural relaxation involves collective, irreversible rearrangements of groups of atoms whose spatial extent is most pronounced at the initial stage of loading and at higher strain amplitudes. At the critical amplitude, the glass becomes mechanically annealed for a number of transient cycles and then yields via the formation of a shear band. The yielding transition is clearly marked by abrupt changes in the potential energy, storage modulus, and fraction of atoms with large nonaffine displacements.

Keywords: yielding transition; metallic glasses; plastic deformation; cyclic loading; molecular dynamics simulations

check for updates

Citation: Priezjev, N.V. Structural Relaxation and Delayed Yielding in Cyclically Sheared Cu-Zr Metallic Glasses. *Metals* **2024**, *14*, 984. https://doi.org/10.3390/met14090984

Academic Editor: Roberto Gomes de Aguiar Veiga

Received: 23 July 2024
Revised: 14 August 2024
Accepted: 25 August 2024
Published: 29 August 2024

Copyright: © 2024 by the authors. Licensee MDPI, Basel, Switzerland. This article is an open access article distributed under the terms and conditions of the Creative Commons Attribution (CC BY) license (https://creativecommons.org/licenses/by/4.0/).

1. Introduction

Establishing structure–property–performance relations for bulk metallic glasses is important for various structural and functional applications [1,2]. Owing to their amorphous atomic structure, metallic glasses offer a number of unique properties, such as high strength, high elastic limit, as well as superior wear and corrosion resistance [3,4]. An outstanding challenge that limits their widespread use is that sufficiently well annealed glasses are prone to brittle failure via the formation of nanoscale shear bands [5]. In addition, metallic glasses subjected to cyclic variations in stresses or strains exhibit relatively low fatigue limit and fatigue life, which can be affected by the sample size, chemical composition, cycling frequency, and surface conditions [6–8]. To enhance their ductility, metallic glasses can be rejuvenated using several thermo-mechanical processing methods, including high-pressure torsion, ion irradiation, thermal cycling, cold rolling, and elastostatic loading [9,10]. Alternatively, an atomic structure can be simply reset by heating above the glass transition temperature and subsequent rapid cooling to the glass state or a supercooled glass former can be frozen under applied stress [11]. In recent years, laser-based additive manufacturing techniques were also introduced to fabricate large-scale complex structures and patient-specific implants for biomedical applications [12]. Despite these advances, however, the development of novel processing methods to rejuvenate metallic glasses and improve their mechanical properties remains a challenging task.

In the last decade, a number of molecular dynamics (MD) simulation studies have investigated the yielding behavior and structural relaxation of amorphous solids subjected to oscillatory deformation [13–37]. Notably, it was demonstrated that in the athermal

limit, binary Lennard–Jones (LJ) glasses under low-amplitude loading gradually evolve into periodic limit cycles with exactly reversible trajectories of atoms [14,16], and the potential energy of such states is lower for better-annealed glasses and higher strain amplitudes [15,21]. In contrast, periodic shear deformation in combination with thermal noise facilitates collective, irreversible rearrangements of atoms and prolonged structural relaxation [31,32]. In addition, lower energy states can be accessed when cyclic shear is periodically alternated along two or three mutually perpendicular planes [25,34]. Moreover, the range of energy states attainable in thermal glasses during low-amplitude loading can be extended by slightly increasing the strain amplitude above a critical point every few cycles [29]. Furthermore, when the loading amplitude exceeds a critical value, amorphous alloys undergo a yielding transition after a number of transient cycles [18,21,23,24,27,32,35]. Interestingly, the critical strain amplitude in athermal systems might depend on the glass stability [26,28], whereas at about half T_g, the yielding transition is delayed in better-annealed glasses but the critical strain amplitude remains unchanged [32]. It was recently shown that well-annealed binary glasses fail via shear band formation, and the number of cycles required to reach the yielding transition is well described by the power-law function of the difference between the strain amplitude and its critical value [35]. However, the role of loading conditions and preparation history on the critical behavior of metallic glasses is not yet fully understood.

In this paper, the yielding behavior and structural relaxation of Cu-Zr metallic glass under periodic shear deformation are studied using molecular dynamics simulations. We consider a binary glass that is first rapidly cooled across the glass transition to room temperature, and then cyclically loaded in a wide range of strain amplitudes around a critical value. It is shown that low-amplitude loading leads to a logarithmic decay of the potential energy during thousands of cycles. When the loading amplitude increases toward the critical value, the average size of plastically deformed domains becomes larger and the glass is relocated to lower energy states. On the contrary, we find that the yielding transition at the critical strain amplitude is marked by abrupt changes in the storage modulus, potential energy, and number of atoms with large nonaffine displacements, which are localized within a narrow shear band.

The rest of this paper is structured as follows. The MD simulation setup, parameter values, and cooling and deformation protocols are described in the next section. Analyses of the potential energy, shear stress, and nonaffine displacements are presented in Section 3. A summary of the results is provided in the last section.

2. MD Simulations

In our study, metallic glass was represented by a binary mixture of Cu and Zr atoms, which interacted via the embedded atom method (EAM) potentials [38,39]. The total number of atoms in the $Cu_{50}Zr_{50}$ glass was 60,000. The preparation procedure consisted of several steps. First, the binary mixture was thoroughly equilibrated in a periodic box at a temperature of 2000 K and under zero pressure in the NPT ensemble using the Nosé–Hoover thermostat. This temperature is well above the glass transition temperature of $T_g \approx 675$ K. We followed the cooling protocol proposed by Fan and Ma [40], where the Cu-Zr system is initially cooled to 1500 K at a rate of 10^{13} K/s, then to 300 K at 10^{12} K/s. As a result, the effective cooling rate was 10^{12} K/s. In the cooling protocol, the temperature was regulated via the Nosé–Hoover thermostat with zero external pressure. Periodic boundary conditions were applied along all three spatial dimensions. Newton's equations of motion were integrated using the velocity Verlet algorithm [41] with a time step of $\triangle t = 1.0$ fs.

Periodic shear deformation was imposed by integration of the SLLOD equations of motion [42] and using the Lees–Edwards periodic boundary conditions along the xz plane as follows:

$$\gamma_{xz}(t) = \gamma_0 \sin(2\pi t/T), \quad (1)$$

where γ_0 is the strain amplitude and T is the oscillation period. In our setup, the oscillation period was set to 1.0 ns (10^6 MD time steps), and the strain amplitude was varied within

the range $0.020 \leqslant \gamma_0 \leqslant 0.061$. The MD simulations were carried out in the NVT ensemble at a temperature of 300 K, and the linear size of the periodic box was 101.8 Å (10.18 nm). A typical simulation of 4000 shear cycles took about 6000 h using 40 processors in parallel. Due to computational limitations, the data for the potential energy, shear stress, and atomic configurations were collected for only one independent sample.

3. Results

One of the key factors that strongly affects the mechanical properties of metallic glasses is the rate of cooling during glass formation [9]. In general, glasses obtained by cooling at a slower rate become more stable and, upon deformation, exhibit a stress overshoot followed by plastic flow, whereas rapidly cooled glasses are settled at higher energy states and yield more smoothly [3]. Alternatively, it was recently demonstrated that poorly annealed LJ glasses can be relocated to lower energy states via low-amplitude cyclic loading at a finite temperature below T_g [31,32]. However, the resulting change in the potential energy at given strain amplitude and temperature as well as the yielding behavior near the critical strain amplitude for more realistic models of glasses remain to be determined. In the present study, we considered the $Cu_{50}Zr_{50}$ glass that was first rapidly cooled to room temperature, then periodically strained for 4000 shear cycles over a broad range of strain amplitudes. This relatively large number of loading cycles was set based on the results of the previous MD study where a rapidly cooled binary LJ glass (60,000 atoms) yielded only after about 2500 cycles at a critical strain amplitude [27].

We first plot potential energy minima after each cycle at zero strain in Figure 1 for strain amplitudes $0.020 \leqslant \gamma_0 \leqslant 0.055$. As is evident, the glass is relocated to progressively lower energy states upon continued loading, and cycle-to-cycle fluctuations are enhanced at higher strain amplitudes. Moreover, cyclic loading at higher strain amplitudes (up to a critical value) allows for the rearrangement of larger clusters of atoms during each cycle, leading, on average, to more relaxed states. These conclusions are in agreement with the results of previous MD studies of binary LJ glasses [21,31,32]. In Figure 2, the same data for the potential energy as a function of the cycle number are replotted on a semi-log scale. It can be clearly observed that for each strain amplitude, the potential energy closely follows a logarithmic decay when $t/T \gtrsim 10$, suggesting the possibility of reaching lower energy states upon further loading. Interestingly, periodic deformation for 4000 shear cycles at $\gamma_0 = 0.055$ resulted in potential energy of $U \approx -4.951$ eV (see Figure 2), which is nearly the same as in the case of a better-annealed $Cu_{50}Zr_{50}$ glass prepared at a 100 times slower cooling rate [35]. In other words, the rapidly cooled glass (10^{12} K/s) was mechanically annealed to the potential energy level of a more slowly cooled glass (10^{10} K/s), which was considered in the previous MD study [35].

The variation of the potential energy during cyclic loading at higher strain amplitudes ($\gamma_0 \geqslant 0.055$) is presented in Figure 3. For reference, the same data for $\gamma_0 = 0.055$ as in Figure 1 are also included in Figure 3 for the first 1300 cycles. It can be readily seen that, following a number of transient cycles, the potential energy abruptly increases, indicating shear band formation at the yielding transition. Note that, except for a relatively high strain amplitude $\gamma_0 = 0.061$, rapidly cooled glass is mechanically annealed for a number of cycles before yielding. The number of cycles required to reach the yielding transition generally increases upon reducing in strain amplitude toward a critical value. As shown in Figure 3, the maximum number of transient cycles is about 650 at the critical strain amplitude $\gamma_0 = 0.056$. The transient behavior can be rationalized as follows. When a rapidly cooled glass is initially strained up to $\gamma_{xz} = \pm\gamma_0$ in Equation (1), the maximum stress remains relatively low and plastic deformation is homogeneously distributed within the sample. Upon further loading, the glass becomes more stable (lower potential energy at zero strain), the maximum stress increases, and the formation of a large-scale plastic event becomes more probable. Finally, we note that a better-annealed $Cu_{50}Zr_{50}$ glass under cyclic loading did not yield for 700 cycles at $\gamma_0 = 0.056$ when the potential energy was

$U \approx -4.951$ eV [35]. Instead, the critical strain amplitude was found to be $\gamma_0 = 0.057$ for similar loading conditions [35].

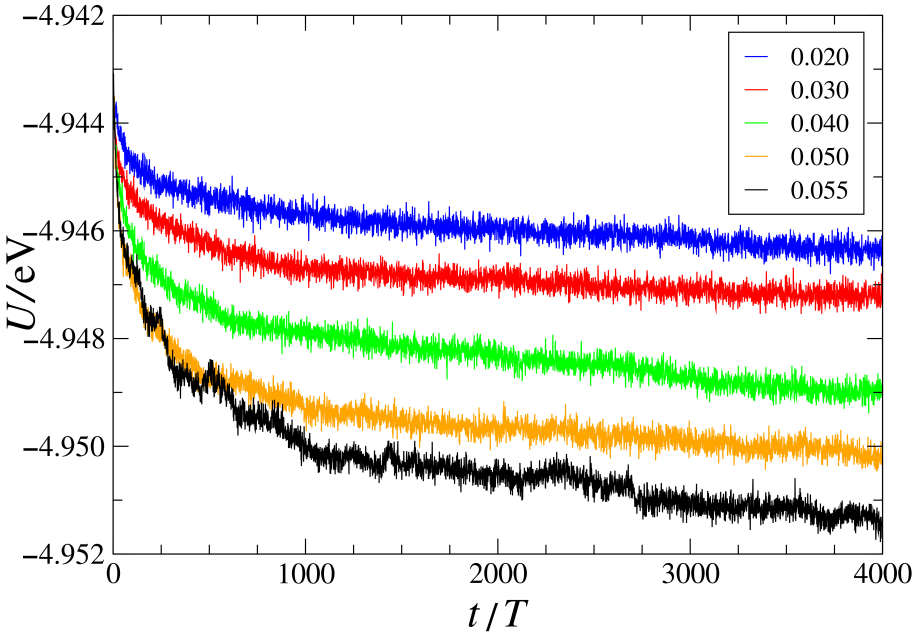

Figure 1. The potential energy at the end of each cycle versus the cycle number for the indicated strain amplitudes (γ_0). The period of oscillation is $T = 1.0$ ns.

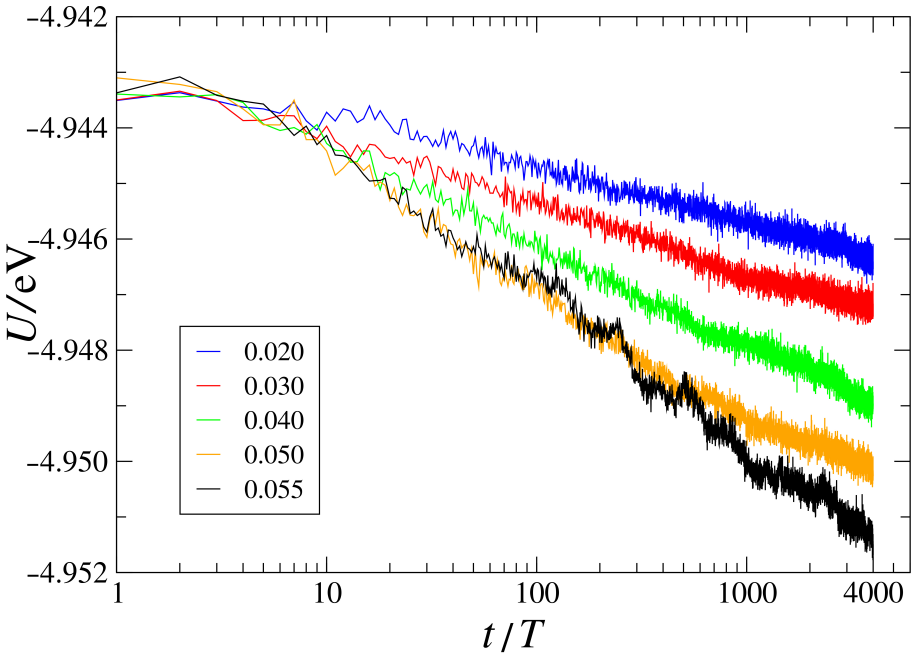

Figure 2. A linear-log plot of the same data as in Figure 1.

Along with the potential energy, the time dependence of shear stress ($\sigma_{xz}(t)$) was analyzed for different strain amplitudes. For each shear cycle, we computed the storage modulus, $G' = \sigma_{xz}^{max}/\gamma_0 \cos(\delta)$, where δ is the phase lag between stress and strain [43]. The variation of the storage modulus is presented in Figure 4 for strain amplitudes below the critical value, i.e., $\gamma_0 \leqslant 0.055$. It can be seen that for each strain amplitude, the storage modulus increases roughly logarithmically as a function of the cycle number, which is consistent with the decay of the potential energy reported in Figure 2. The largest increase in G' during 4000 cycles is found for a strain amplitude of $\gamma_0 = 0.055$, which is just below

the critical value (see Figure 4). Similar to the results for binary LJ glasses [23], the storage modulus is larger for cyclic loading at lower strain amplitudes, where deviation from the elastic regime of deformation is reduced.

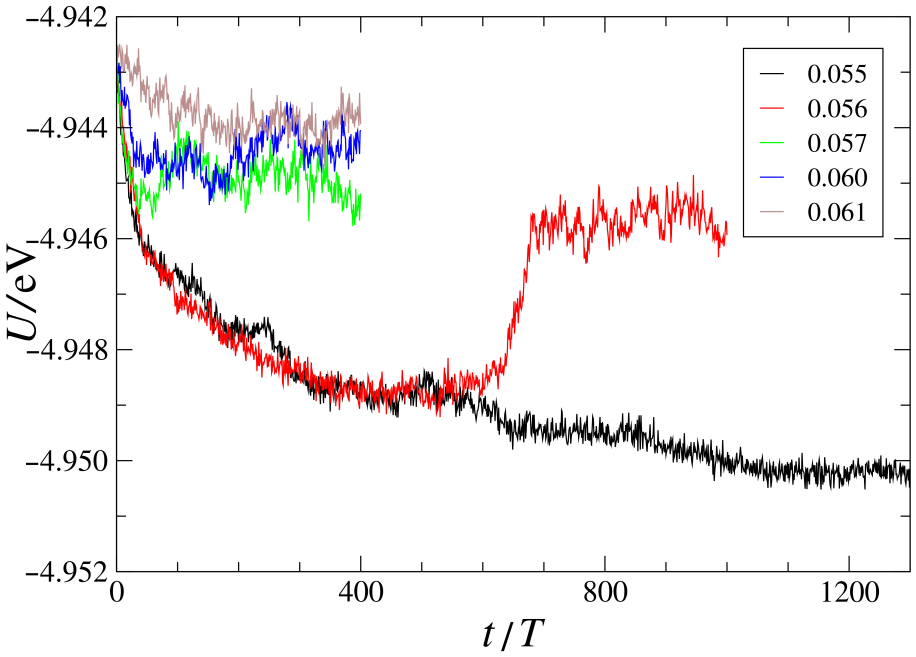

Figure 3. The variation of potential energy when strain is zero as a function of the number of cycles for strain amplitudes of $\gamma_0 = 0.055$, 0.056, 0.057, 0.060, and 0.061. The data for $\gamma_0 = 0.055$ are the same as in Figure 1.

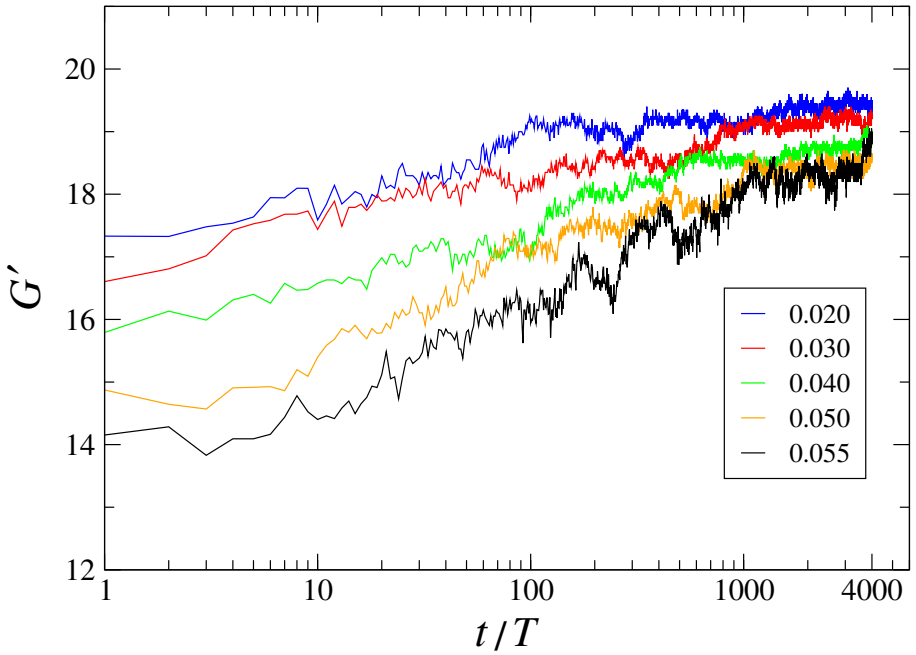

Figure 4. The storage modulus (G', in units of GPa) as a function of the cycle number for the indicated values of the strain amplitude (γ_0). The period of oscillation is $T = 1.0$ ns.

Next, we examine the stress–strain response of binary glass subjected to startup continuous shear deformation with a constant strain rate of 10^{-5} ps^{-1}. The dependence of shear stress as a function of strain is shown in Figure 5 after loading for 4000 cycles at the indicated strain amplitudes. For comparison, the data for the glass after rapid cooling but

before cyclic deformation are also included in Figure 5. As expected, the rapidly cooled glass under steady strain exhibits a smooth crossover to plastic flow (the violet curve in Figure 5). In contrast, plastic flow of mechanically annealed glasses is preceded by the yielding peak, which becomes more pronounced in glasses previously loaded at higher strain amplitudes. In Figure 6, we summarize results for the shear modulus, as computed from the slope of the stress–strain curves at $\gamma_{xz} \leqslant 0.01$, and the peak value of the stress overshoot as functions of the strain amplitude and the potential energy after 4000 cycles. It can be concluded from Figure 6b that the potential energy of the mechanically annealed glass is approximately linearly related to the magnitude of the yielding peak. On the other hand, the shear modulus remains rather insensitive to the loading amplitude, as shown Figure 6c. For completeness, we also present a weak dependence of G on the potential energy after 4000 loading cycles in Figure 6d as well as a monotonic increase of σ_Y on the strain amplitude in Figure 6a.

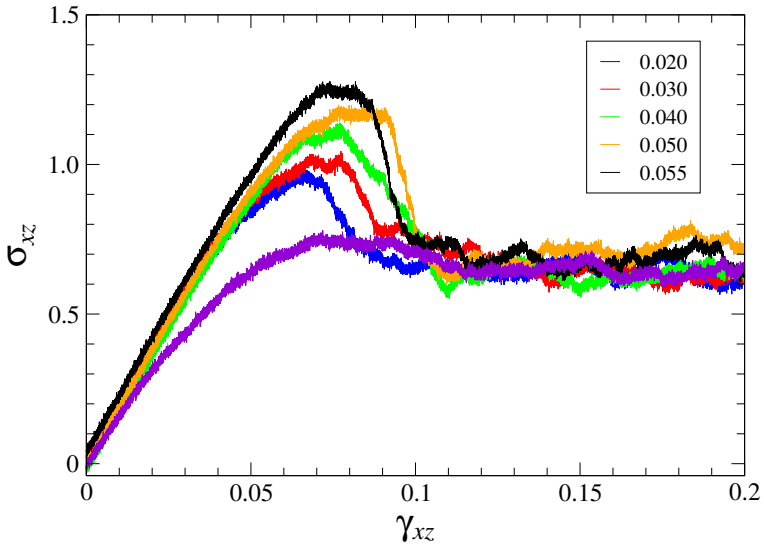

Figure 5. Shear stress (σ_{xz}, in units of GPa), versus strain for glasses deformed at a constant strain rate of 10^{-5} ps^{-1} after 4000 cycles at the indicated γ_0. The lower violet curve represents data before cyclic loading.

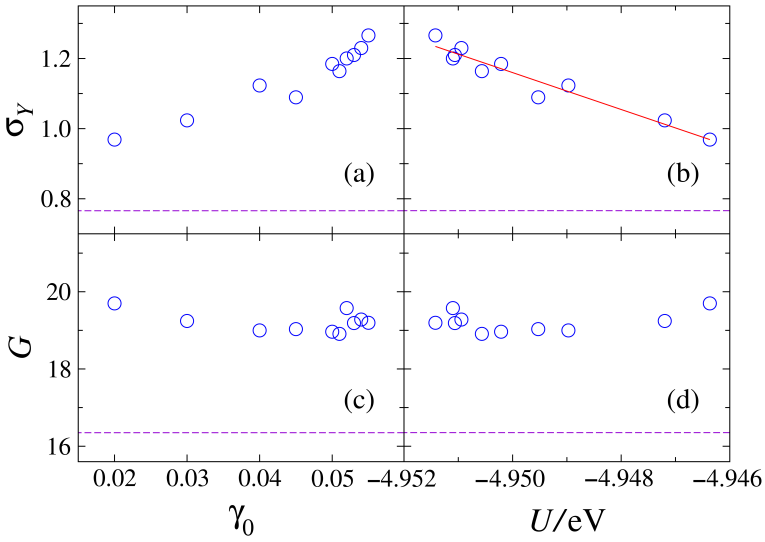

Figure 6. The shear modulus (G, in GPa) and the peak value of the stress overshoot (σ_Y, in GPa) as functions of the strain amplitude (γ_0) and the potential energy after 4000 loading cycles (U). The horizontal dashed lines indicate G and σ_Y for the steadily sheared glass before cyclic loading was applied. The straight red line in the panel (**b**) is the best fit to the data (R^2 = 0.94).

The storage modulus as a function of the cycle number is plotted in Figure 7 for $\gamma_0 \geqslant 0.055$. Note that the data for a strain amplitude of $\gamma_0 = 0.055$ are the same as in Figure 4. It is seen in Figure 7 that in the range $0.056 \leqslant \gamma_0 \leqslant 0.060$, cyclic loading leads to an increase in G' for a number of transient cycles, followed by the yielding transition, which is marked by an abrupt drop in storage modulus. Interestingly, the storage modulus as a function of the cycle number at the critical strain amplitude, i.e., $\gamma_0 = 0.056$, closely follows the data for $\gamma_0 = 0.055$ during the first 600 cycles. Thus, the onset of yielding cannot be determined from the stress variation during the initial stage of deformation near the critical strain amplitude. As shown in Figure 7, the number of transient cycles is reduced at higher strain amplitudes ($\gamma_0 > 0.056$). Overall, these results correlate well with dependence of the potential energy minima on the number of cycles reported in Figure 3.

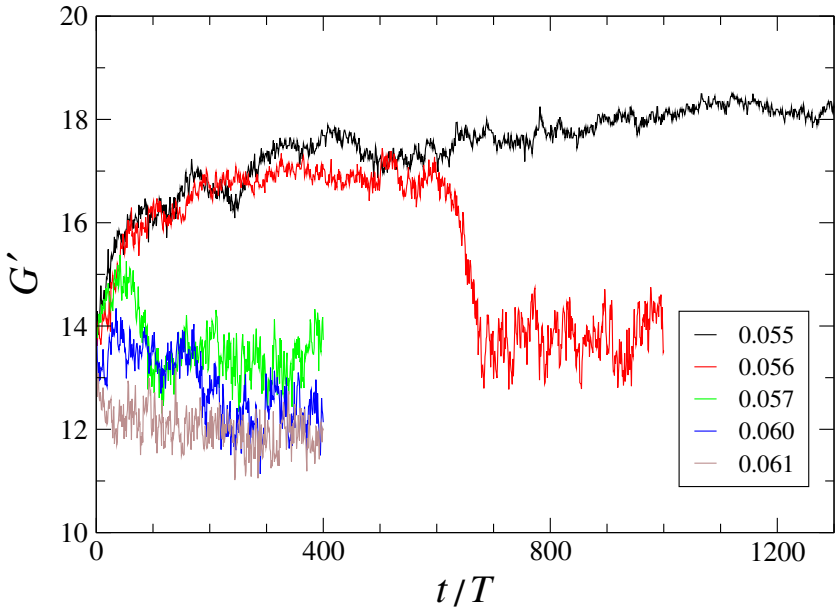

Figure 7. The storage modulus (G' in units of GPa) versus the cycle number for strain amplitudes $\gamma_0 \geqslant 0.055$. The data for G' at $\gamma_0 = 0.055$ are the same as in Figure 4. The oscillation period is $T = 1.0$ ns.

At the microscopic level, plastic deformation in disordered materials can be described via the so-called nonaffine displacements of atoms with respect to their neighbors [44]. In practice, the nonaffine quantity for an atom displaced from the position vector $\mathbf{r}_i(t)$ to $\mathbf{r}_i(t + \Delta t)$ during the time interval of Δt is computed by minimizing the following expression:

$$D^2(t, \Delta t) = \frac{1}{N_i} \sum_{j=1}^{N_i} \left\{ \mathbf{r}_j(t + \Delta t) - \mathbf{r}_i(t + \Delta t) - \mathbf{J}_i \left[\mathbf{r}_j(t) - \mathbf{r}_i(t) \right] \right\}^2, \quad (2)$$

where $\mathbf{J}_i$ is the transformation matrix and the sum is taken over neighboring atoms that are initially located within 4.0 Å from $\mathbf{r}_i(t)$. It was recently shown that in glasses under periodic deformation, rearrangements of atoms become irreversible when their nonaffine displacements are greater than a cage size [19]. In addition, previous MD simulation study has indicated that the cage size is about 0.6 Å for $Cu_{50}Zr_{50}$ metallic alloy near the glass transition temperature [45].

The dependence of the nonaffine measure as a function of the cycle number is presented in Figure 8 for $\gamma_0 \leqslant 0.055$ and in Figure 9 for $\gamma_0 \geqslant 0.055$. In our analysis, the nonaffine measure was computed at the beginning and end of each cycle, $\Delta t = T$ in Equation (2), and then averaged over all atoms. For cyclic loading below the critical strain amplitude, $\gamma_0 = 0.056$, the glass evolves toward lower energy states via a sequence of plastic events, whose size is reduced at lower amplitudes, and, as a result, the average of D^2 is smaller at

lower γ_0 values, as shown in Figure 8. Note that the largest fluctuations in D^2 occur at a strain amplitude of $\gamma_0 = 0.055$, whereas the lower bound, $D^2 \approx 0.1\,\text{Å}^2$, is dominated by displacements of atoms within their cages. Furthermore, the results presented in the inset of Figure 8 for the fraction of atoms with large nonaffine displacements clearly demonstrate that the number of atoms involved in plastic events decays with increasing number of cycles. In contrast, the average of D^2 increases sharply at the yielding transition for $\gamma_0 \geqslant 0.056$ (see Figure 9), which is in agreement with the critical behavior of U and G' reported in Figures 3 and 7, respectively. Moreover, after the yielding transition, plastic flow is localized within a shear band that contains a large fraction of atoms ($n_f \gtrsim 0.25$) (see Figure 10).

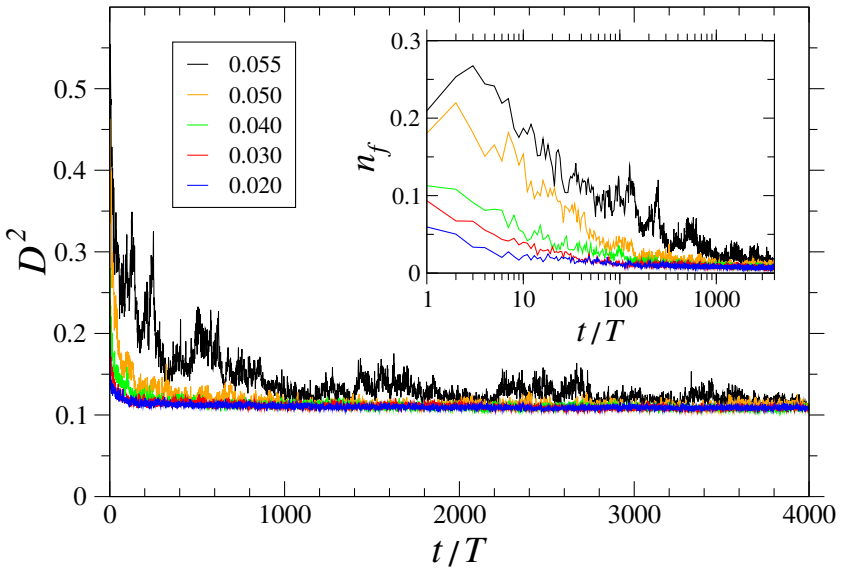

Figure 8. The average of the nonaffine quantity ($D^2[(n-1)\,T, T]$, in units of Å^2) as a function of the number of cycles for the indicated strain amplitudes. The oscillation period is $T = 1.0$ ns. The inset shows the fraction of atoms with $D^2[(n-1)\,T, T] > 0.49\,\text{Å}^2$ versus the cycle number for the same strain amplitudes.

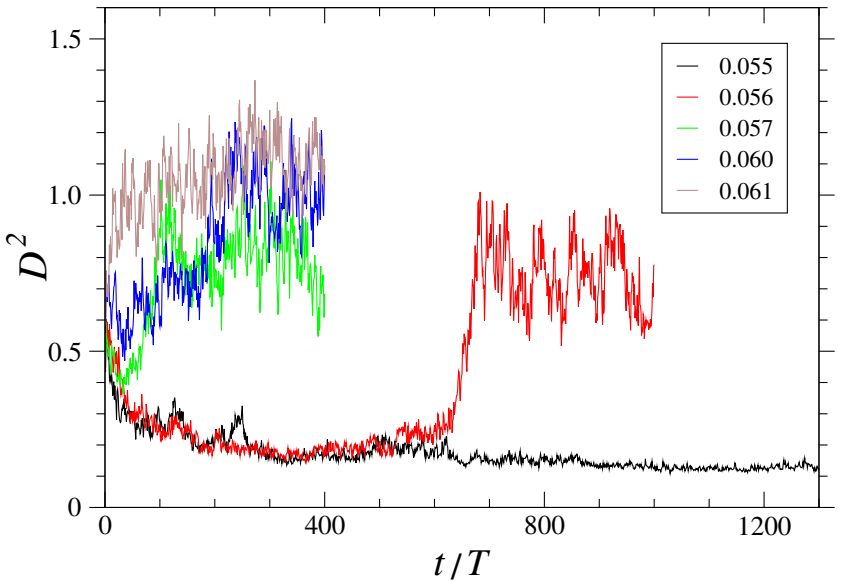

Figure 9. The average of $D^2[(n-1)\,T, T]$ (in units of Å^2) versus the number of cycles for strain amplitudes of $\gamma_0 \geqslant 0.055$. The data for the strain amplitude of $\gamma_0 = 0.055$ (the black curve) are the same as in Figure 8.

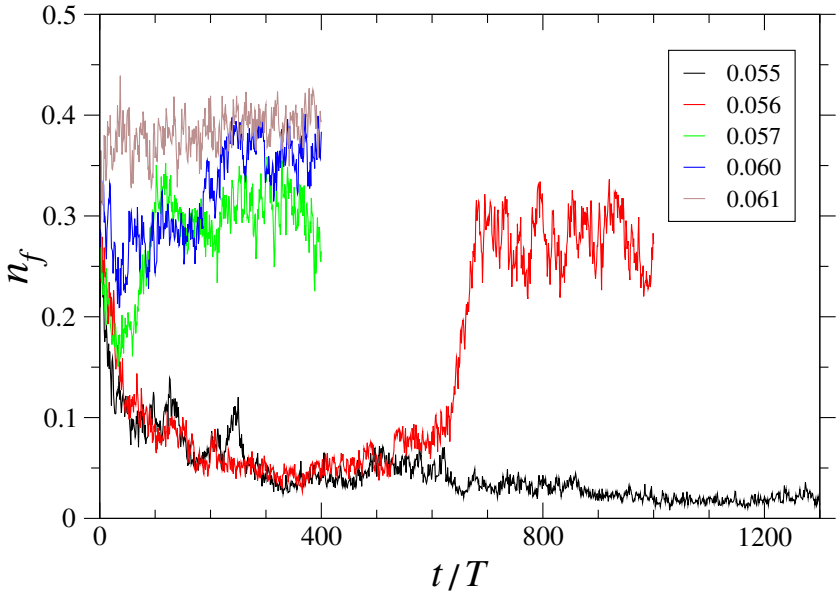

Figure 10. The fraction of atoms with large nonaffine displacements ($D^2[(n-1)\,T, T] > 0.49\,\text{Å}^2$) as a function of the number of cycles for the tabulated strain amplitudes. The oscillation period is $T = 1.0\,\text{ns}$.

The spatial organization of plastically deformed domains during the relaxation process at a strain amplitude of $\gamma_0 = 0.055$ is illustrated in Figure 11. The snapshots include configurations of atoms after n cycles at zero strain, and the color code denotes the magnitude of the nonaffine measure for $\Delta t = T$ in Equation (2). Note that atoms with relatively small nonaffine displacements ($D^2[(n-1)\,T, T] < 0.49\,\text{Å}^2$) were omitted for clarity, and, therefore, the void space represents elastically deformed regions. As shown in Figure 11a, the transition to lower energy states initially proceeds via large, irreversible displacements of atoms that form several compact clusters homogeneously distributed in the sample. Upon further loading, the total number of atoms with large nonaffine displacements is significantly reduced (see Figure 11b), and eventually, plastic rearrangements remain localized only in several isolated clusters (see Figure 11c,d). Hence, these results demonstrate that poorly annealed glasses subjected to prolonged low-amplitude periodic deformation become more stable and reversible. On the contrary, cyclic loading at the critical strain amplitude, i.e., $\gamma_0 = 0.056$, leads to a delayed yielding transition and the formation of a shear band across the whole sample, as shown in Figure 12. A close comparison of the results for $\gamma_0 = 0.056$ in Figures 10 and 12 reveals details of the yielding transition, namely, shear band initiation [$n_f = 0.07$ in Figure 12b], propagation of plastic regions along the yz plane [$n_f = 0.20$ in Figure 12c], and formation of a fully developed shear band [$n_f = 0.28$ in Figure 12d]. Together, these findings emphasize the role of plastic rearrangements in structural relaxation and yielding of metallic glasses under cyclic loading.

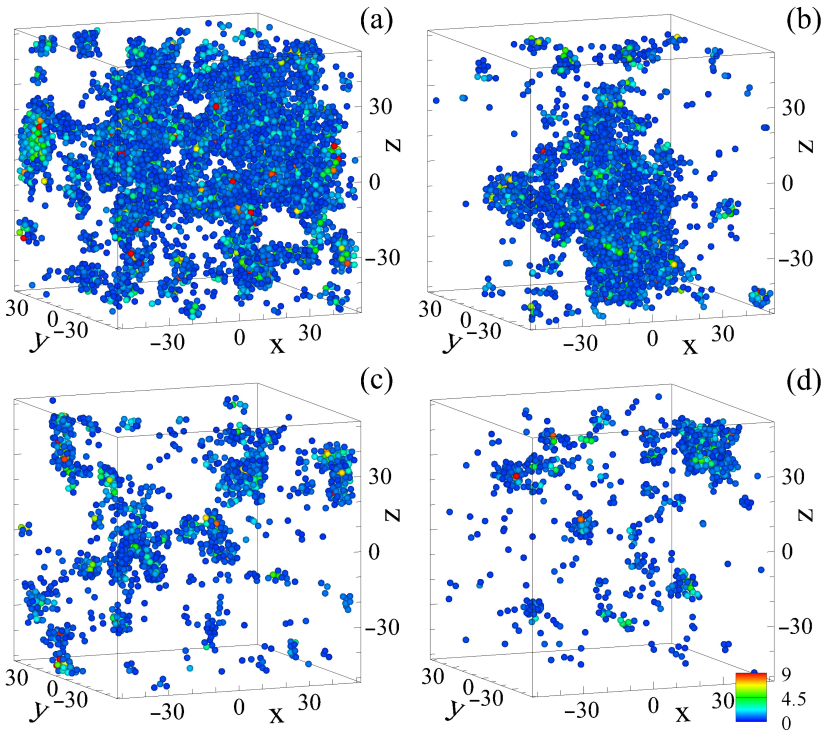

Figure 11. Selected configurations of atoms in $Cu_{50}Zr_{50}$ glass loaded at a strain amplitude of $\gamma_0 = 0.055$. The nonaffine quantity is (**a**) $D^2(50\,T, T) > 0.49\,\text{Å}^2$, (**b**) $D^2(500\,T, T) > 0.49\,\text{Å}^2$, (**c**) $D^2(1000\,T, T) > 0.49\,\text{Å}^2$, and (**d**) $D^2(3000\,T, T) > 0.49\,\text{Å}^2$. Cu and Zr atoms are not drawn to scale. The legend in panel (**d**) indicates the magnitude of the nonaffine quantity.

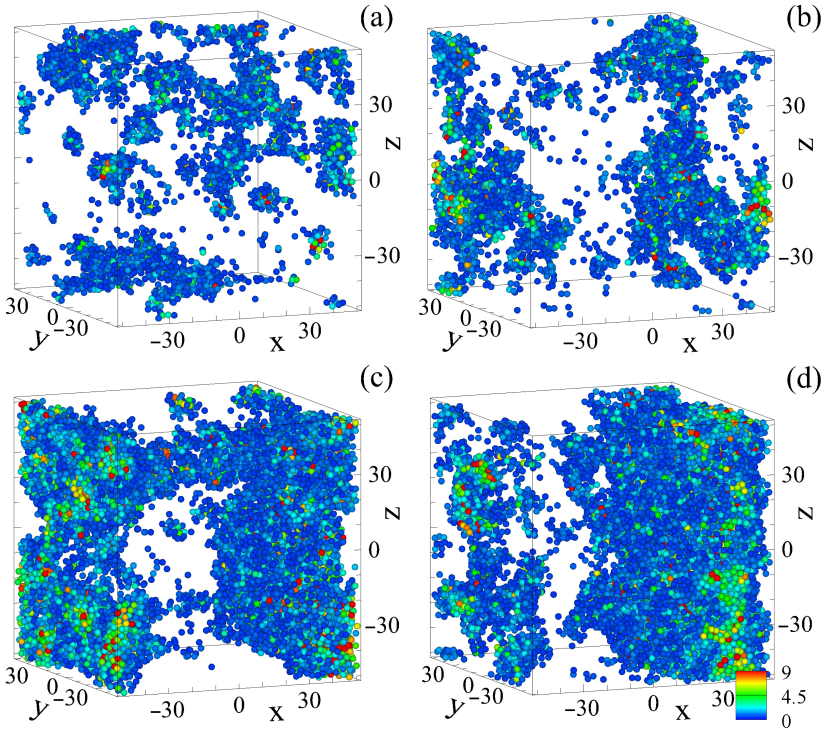

Figure 12. Snapshots of atomic configurations of the binary glass periodically deformed at the critical strain amplitude of $\gamma_0 = 0.056$. The nonaffine measure is (**a**) $D^2(300\,T, T) > 0.49\,\text{Å}^2$, (**b**) $D^2(600\,T, T) > 0.49\,\text{Å}^2$, (**c**) $D^2(660\,T, T) > 0.49\,\text{Å}^2$, and (**d**) $D^2(800\,T, T) > 0.49\,\text{Å}^2$. Atoms are not depicted to scale. The color code is the same as in Figure 11.

4. Conclusions

In summary, we investigated the critical behavior and mechanical annealing of Cu-Zr metallic glass subjected to periodic shear deformation by means of molecular dynamics simulations. The glass was prepared via rapid cooling from the liquid state to room temperature, then subjected to oscillatory shear at strain amplitudes ranging from slightly above to well below a critical value. It was found that low-amplitude cyclic loading gradually relocates the glass to lower energy states, and the storage modulus approximately follows a logarithmic dependence on the number of shear cycles. In addition, we showed that the potential energy after four thousand shear cycles depends linearly on the yielding stress of the annealed glass under monotonic shear deformation. Structural relaxation proceeds via a sequence of plastic rearrangements of clusters of atoms whose typical size is larger at higher strain amplitudes. In contrast, when the strain amplitude is greater than a critical value, the glass is mechanically annealed for a number of cycles, followed by an abrupt increase in the potential energy due to flow localization within a shear band. The formation of the shear band is accompanied by an increase in the fraction of atoms with large nonaffine displacements and a drop in storage modulus.

Funding: This work was supported by National Science Foundation [CNS-1531923].

Data Availability Statement: The raw data supporting the conclusions of this article will be made available by the authors on request.

Acknowledgments: MD simulations were carried out at Wright State University's Computing Facility and the Ohio Supercomputer Center using the LAMMPS code [41].

Conflicts of Interest: The author declares that he has no conflict of interest.

References

1. Gao, K.; Zhu, X.G.; Chen, L.; Li, W.H.; Xu, X.; Pan, B.T.; Li, W.R.; Zhou, W.H.; Li, L.; Huang, W.; et al. Recent development in the application of bulk metallic glasses. *J. Mater. Sci. Technol.* **2022**, *131*, 115–121. [CrossRef]
2. Jiang, H.; Shang, T.; Xian, H.; Sun, B.; Zhang, Q.; Yu, Q.; Bai, H.; Gu, L.; Wang, W. Functional properties of amorphous alloys. *Small Struct.* **2021**, *2*, 2000057. [CrossRef]
3. Egami, T.; Iwashita, T.; Dmowski, W. Mechanical properties of metallic glasses. *Metals* **2013**, *3*, 77–113. [CrossRef]
4. Qiao, J.C.; Wang, Q.; Pelletier, J.M.; Kato, H.; Casalini, R.; Crespo, D.; Pineda, E.; Yao, Y.; Yang, Y. Structural heterogeneities and mechanical behavior of amorphous alloys. *Prog. Mater. Sci.* **2019**, *104*, 250–329. [CrossRef]
5. Hufnagel, T.C.; Schuh, C.A.; Falk, M.L. Deformation of metallic glasses: Recent developments in theory, simulations, and experiments. *Acta Mater.* **2016**, *109*, 375–393. [CrossRef]
6. Jia, H.; Wang, G.; Chen, S.; Gao, Y.; Li, W.; Liaw, P.K. Fatigue and fracture behavior of bulk metallic glasses and their composites. *Prog. Mater. Sci.* **2018**, *98*, 168–248. [CrossRef]
7. Menzel, B.C.; Dauskardt, R.H. Stress-life fatigue behavior of a Zr-based bulk metallic glass. *Acta Mater.* **2006**, *54*, 935–943. [CrossRef]
8. Sha, Z.; Lin, W.; Poh, L.H.; Xing, G.; Liu, Z.; Wang, T.; Gao, H. Fatigue of metallic glasses. *Appl. Mech. Rev.* **2020**, *72*, 050801. [CrossRef]
9. Sun, Y.; Concustell, A.; Greer, A.L. Thermomechanical processing of metallic glasses: Extending the range of the glassy state. *Nat. Rev. Mater.* **2016**, *1*, 16039. [CrossRef]
10. Ketov, S.V.; Sun, Y.H.; Nachum, S.; Lu, Z.; Checchi, A.; Beraldin, A.R.; Bai, H.Y.; Wang, W.H.; Louzguine-Luzgin, D.V.; Carpenter, M.A.; et al. Rejuvenation of metallic glasses by non-affine thermal strain. *Nature* **2015**, *524*, 200–203. [CrossRef]
11. Mota, R.M.O.; Lund, E.T.; Sohn, S.; Browne, D.J.; Hofmann, D.C.; Curtarolo, S.; van de Walle, A.; Schroers, J. Enhancing ductility in bulk metallic glasses by straining during cooling. *Commun. Mater.* **2021**, *2*, 23. [CrossRef]
12. Aliyu, A.A.A.; Panwisawas, C.; Shinjo, J.; Puncreobutr, C.; Reed, R.C.; Poungsiri, K.; Lohwongwatana, B. Laser-based additive manufacturing of bulk metallic glasses: Recent advances and future perspectives for biomedical applications. *J. Mater. Res. Technol.* **2023**, *23*, 2956–2990. [CrossRef]
13. Priezjev, N.V. Heterogeneous relaxation dynamics in amorphous materials under cyclic loading. *Phys. Rev. E* **2013**, *87*, 052302. [CrossRef] [PubMed]
14. Regev, I.; Lookman, T.; Reichhardt, C. Onset of irreversibility and chaos in amorphous solids under periodic shear. *Phys. Rev. E* **2013**, *88*, 062401. [CrossRef]
15. Fiocco, D.; Foffi, G.; Sastry, S. Oscillatory athermal quasistatic deformation of a model glass. *Phys. Rev. E* **2013**, *88*, 020301. [CrossRef]

16. Regev, I.; Weber, J.; Reichhardt, C.; Dahmen, K.A.; Lookman, T. Reversibility and criticality in amorphous solids. *Nat. Commun.* **2015**, *6*, 8805. [CrossRef]
17. Luo, J.; Dahmen, K.; Liaw, P.K.; Shi, Y. Low-cycle fatigue of metallic glass nanowires. *Acta Mater.* **2015**, *87*, 225–232. [CrossRef]
18. Sha, Z.D.; Qu, S.X.; Liu, Z.S.; Wang, T.J.; Gao, H. Cyclic deformation in metallic glasses. *Nano Lett.* **2015**, *15*, 7010–7015. [CrossRef]
19. Priezjev, N.V. Reversible plastic events during oscillatory deformation of amorphous solids. *Phys. Rev. E* **2016**, *93*, 013001. [CrossRef]
20. Kawasaki, T.; Berthier, L. Macroscopic yielding in jammed solids is accompanied by a non-equilibrium first-order transition in particle trajectories. *Phys. Rev. E* **2016**, *94*, 022615. [CrossRef]
21. Leishangthem, P.; Parmar, A.D.S.; Sastry, S. The yielding transition in amorphous solids under oscillatory shear deformation. *Nat. Commun.* **2017**, *8*, 14653. [CrossRef]
22. Dagois-Bohy, S.; Somfai, E.; Tighe, B.P.; van Hecke, M. Softening and yielding of soft glassy materials. *Soft Matter* **2017**, *13*, 9036–9045. [CrossRef] [PubMed]
23. Priezjev, N.V. The yielding transition in periodically sheared binary glasses at finite temperature. *Comput. Mater. Sci.* **2018**, *150*, 162–168. [CrossRef]
24. Parmar, A.D.S.; Kumar, S.; Sastry, S. Strain localization above the yielding point in cyclically deformed glasses. *Phys. Rev. X* **2019**, *9*, 021018. [CrossRef]
25. Priezjev, N.V. Accelerated relaxation in disordered solids under cyclic loading with alternating shear orientation. *J. Non-Cryst. Solids* **2019**, *525*, 119683. [CrossRef]
26. Yeh, W.T.; Ozawa, M.; Miyazaki, K.; Kawasaki, T.; Berthier, L. Glass stability changes the nature of yielding under oscillatory shear. *Phys. Rev. Lett.* **2020**, *124*, 225502. [CrossRef]
27. Priezjev, N.V. Alternating shear orientation during cyclic loading facilitates yielding in amorphous materials. *J. Mater. Eng. Perform.* **2020**, *29*, 7328–7335. [CrossRef]
28. Bhaumik, H.; Foffi, G.; Sastry, S. The role of annealing in determining the yielding behavior of glasses under cyclic shear deformation. *Proc. Natl. Acad. Sci. USA* **2021**, *118*, e2100227118. [CrossRef]
29. Priezjev, N.V. Accessing a broader range of energy states in metallic glasses by variable-amplitude oscillatory shear. *J. Non-Cryst. Solids* **2021**, *560*, 120746. [CrossRef]
30. Cui, S.; Liu, H.; Peng, H. Anisotropic correlations of plasticity on the yielding of metallic glasses. *Phys. Rev. E* **2022**, *106*, 014607. [CrossRef]
31. Das, P.; Parmar, A.D.S.; Sastry, S. Annealing glasses by cyclic shear deformation. *J. Chem. Phys.* **2022**, *157*, 044501. [CrossRef] [PubMed]
32. Priezjev, N.V. Mechanical annealing and yielding transition in cyclically sheared binary glasses. *J. Non-Cryst. Solids* **2022**, *590*, 121697. [CrossRef]
33. Shang, B.; Jakse, N.; Guan, P.; Wang, W.; Barrat, J.-L. Influence of oscillatory shear on nucleation in metallic glasses: A molecular dynamics study. *Acta Mater.* **2023**, *246*, 118668. [CrossRef]
34. Krishnan, V.V.; Ramola, K.; Karmakar, S. Annealing effects of multidirectional oscillatory shear in model glass formers. *Phys. Rev. Appl.* **2023**, *19*, 024004. [CrossRef]
35. Priezjev, N.V. Fatigue behavior of Cu-Zr metallic glasses under cyclic loading. *Metals* **2023**, *13*, 1606. [CrossRef]
36. Zella, L.; Moon, J.; Egami, T. Ripples in the bottom of the potential energy landscape of metallic glass. *Nat. Commun.* **2024**, *15*, 1358. [CrossRef]
37. Tang, X.C.; Yao, X.H. The effect of forced vibration coupling on amorphous alloy superplasticity. *J. Non-Cryst. Solids* **2024**, *630*, 122905. [CrossRef]
38. Cheng, Y.Q.; Ma, E.; Sheng, H.W. Atomic level structure in multicomponent bulk metallic glass. *Phys. Rev. Lett.* **2009**, *102*, 245501. [CrossRef] [PubMed]
39. Cheng, Y.Q.; Ma, E. Atomic-level structure and structure-property relationship in metallic glasses. *Prog. Mater. Sci.* **2011**, *56*, 379. [CrossRef]
40. Fan, Z.; Ma, E. Predicting orientation-dependent plastic susceptibility from static structure in amorphous solids via deep learning. *Nat. Commun.* **2021**, *12*, 1506. [CrossRef]
41. Plimpton, S.J. Fast parallel algorithms for short-range molecular dynamics. *J. Comput. Phys.* **1995**, *117*, 1–19. [CrossRef]
42. Evans, D.J.; Morriss, G.P. Nonlinear-response theory for steady planar Couette flow. *Phys. Rev. A* **1984**, *30*, 1528. [CrossRef]
43. Hyun, K.; Wilhelm, M.; Klein, C.O.; Cho, K.S.; Nam, J.G.; Lee, S.J.; Ewoldt, R.H.; McKinley, G.H. A review of nonlinear oscillatory shear tests: Analysis and application of large amplitude oscillatory shear (LAOS). *Prog. Polym. Sci.* **2011**, *36*, 1697–1753. [CrossRef]
44. Falk, M.L.; Langer, J.S. Dynamics of viscoplastic deformation in amorphous solids. *Phys. Rev. E* **1998**, *57*, 7192. [CrossRef]
45. Wang, X.; Xu, W.-S.; Zhang, H.; Douglas, J.F. Universal nature of dynamic heterogeneity in glass-forming liquids: A comparative study of metallic and polymeric glass-forming liquids. *J. Chem. Phys.* **2019**, *151*, 184503. [CrossRef]

Disclaimer/Publisher's Note: The statements, opinions and data contained in all publications are solely those of the individual author(s) and contributor(s) and not of MDPI and/or the editor(s). MDPI and/or the editor(s) disclaim responsibility for any injury to people or property resulting from any ideas, methods, instructions or products referred to in the content.